Available online at www.sciencedirect.com
SCIENCE DIRECT®
Spectrochimica Acta Part A xxx (2003) xxx–xxx
SPECTROCHIMICA ACTA PART A
www.elsevier.com/locate/saa

Complexing properties of nucleic-acid constituents adenine and guanine complexes

Mamdouh S. Masoud [a,*], Amina A. Soayed [a], Alaa E. Ali [b]

[a] Chemisty Department, Faculty of Science, Alexandria University, Alexandria, Egypt
[b] Physics and Chemistry Department, Faculty of Education, Damanhour, Alexandria University, Alexandria, Egypt

Received 19 August 2003; received in revised form 14 September 2003; accepted 30 September 2003

Abstract

Cobalt, nickel and copper complexes of adenine and guanine, as nucleic-acid constituents, were prepared. The adenine and guanine complexes are of tetrahedral and octahedral geometries, respectively. All are of high spin nature. The nickel complexes are of 2:1 metal:ligand ratio with Ni · · · Ni direct interaction in the guanine complex. The coordination bonds of adenine metal complexes are calculated and follow the order: Cu^{II}-adenine < Ni^{II}-adenine < Co^{I}-adenine. The Cu^{II}-adenine complex is the stronger following the softness of the copper, while that of guanine is less covalent. The copper complexes are with stronger axial field. The differential thermal analysis (DTA) and TGA of the complexes pointed to their stability. The mechanism of the thermal decomposition is detected. The thermodynamic parameters of the dissociation steps are evaluated. The complexes are of semi-conducting behaviour for their technical applications. Empirical equations are deduced between the electrical conducting and the energy of activation of the complexes.

Keywords: Nucleic acid complexes; Magnetism; Spectroscopy; Thermal; Electrical conductivity

1. Introduction

Nucleic acids and their derivatives are natural multisided ligands. The interaction of these molecules with both natural and foreign metal species has stimulated great interest for many reasons [1–4]: (1) enzyme reactions that require nucleic-acid constituents; (2) enzyme reactions that act on these compounds; (3) the structures of nucleic acids in vivo; and (4) the structures of nucleic acid–protein complexes. The key of studying these important aspects is to study the complexing properties of the nucleic-acid constituents with different metal ions in a sequel of continuation. Masoud and others [5–14] reported the complexing properties of some biologically active pyrimidine compounds. In continuation, purines (adenine and guanine) complexes of cobalt, nickel and copper ions are the major goal of the present work. The study includes spectral (UV-Vis, IR, ESR), magnetic susceptibility, thermal and electrical properties to shed light on their structural chemistry.

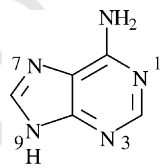

Adenine (HL)

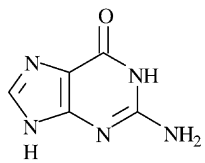

Guanine (H_2L')

2. Experimental

2.1. Preparation of the complexes

Amnoniacal solutions of 0.01 mol cobalt(II), nickel(II) and copper(II) chlorides were mixed with 0.02 mol of adenine or guanine previously dissolved in ammonia solution. The reaction mixture was refluxed for two hours and then left overnight where the complexes were precipitated, then filtered, washed with distilled water and dried in a vacuum desicator over P_4O_{10}. The melting points of the complexes are over 300 °C.

* Corresponding author.
E-mail address: drmsmasoud@yahoo.com (M.S. Masoud).

1386-1425/$ – see front matter © 2003 Published by Elsevier B.V.
doi:10.1016/j.saa.2003.09.025

2.2. Analysis of metal ion content

The complexes were digested and decomposed with aquaregia. The metal ion contents were determined by usual complexmetric procedures [15].

2.3. Carbon, hydrogen and nitrogen analyses

These were done at the Micro Analytical Laboratory, Faculty of Science, Alexandria University, Egypt.

2.4. Halogen analysis

It was determined by titration with standard $Hg(NO_3)_2$ solution using diphenylcarbazone indicator [15]. The analytical data, colours of the prepared complexes are collected in Table 1.

2.5. Instruments and working procedures

2.5.1. UV-Vis spectra

The spectral studies were measured using PYE-Unicam spectrophotometer model 1750 covering the wavelength range 190–900 mm. The complexes were measured in Nujol mull following the method described by Lee et al. [16].

2.5.2. IR spectra

The KBr IR spectra were recorded using Perkin-Elmer spectrophotometer model 1430 covering the frequency range 200–4000 cm^{-1}. Calibration of the frequency readings was made with polystyrene film.

2.5.3. ESR spectra

ESR spectra were recorded at 100 kHz modulation and 10 G modulation amplitude on Varian E-9 Spectrophotometer. Incident power of 10 mV was used and resonance conditions were at ca 9.75 GHz (X-band) at room temperature. Spectra were obtained with an air products LTD-3-110 Heli-Trans liquid helium transfer refrigerator. The field was calibrated with a powder sample of 2,2-diphenyl pyridylhydrazone (DPPH) $g = 2.0037$ [17].

2.6. Magnetic susceptibility measurements

Molar magnetic susceptibility corrected for diamagnetic using Pascal's constant were determined at room temperature (298 K) using Faraday's method. The apparatus was calibrated with Hg $[Co(SCN)_4]$ [18].

2.7. Thermal analysis

Differential thermal analysis (DTA) was carried out using a Schimatzu DTA-50. The rate of heating was 10 °C min^{-1}.

2.8. Electrical conductivity

The dc electrical conductivity measurements of the solid complexes were taken in air on keithley multimeter with applied voltage 200 V using two probe method. The discs were pressed under 5 t cm^{-2} to a thickness of 0.1–0.3 cm. The tablets were covered on both sites with sliver paste to improve the contact with the electrodes. The conductivity was measured in the temperature range 298–643 °K with a stability and accuracy of ±0.1 K. The dc electrical conductivity was calculated using the general equation:

$$\sigma = \frac{I}{V_c}\frac{d}{a}$$

where I is the current in ampere and V_c is the potential drop across the sample of the cross-section area a and thickness d.

3. Results and discussion

3.1. Spectral and magnetic identification of adenine complexes

The IR spectra of adenine and its metal complexes have been studied by several research groups [19–22]. Certain band assignments, especially those concerning with NH_2 modes at 1260–1020 cm^{-1}, differ from work to work [19–22]. The NH_2 bands of adenine at 3286 and 3114 cm^{-1} (Table 2) are slightly shifted on complexation. The δ_{NH2} mode of the free adenine at 1668 cm^{-1} undergoes shifts

Table 1
Analytical data and colour of the purine complexes

Complex	Colour	Calculated (found) (%)				
		C	H	N	M	Cl
Co-adenine	Black	24.36 (24.21)	2.45 (2.36)	28.41 (28.32)	23.91 (23.87)	14.38 (14.27)
Ni-adenine	Pale green	15.98 (15.80)	1.61 (1.61)	18.63 (18.60)	31.23 (31.22)	28.29 (28.31)
Cu-adenine	Green	23.91 (23.95)	2.41 (2.40)	27.89 (27.95)	25.30 (25.29)	14.12 (14.10)
Co-guanine	Beige	30.30 (30.37)	3.80 (3.76)	32.80 (32.58)	12.40 (12.39)	7.50 (7.49)
Ni-guanine	Pale green	29.20 (29.18)	3.40 (3.42)	30.01 (29.07)	16.80 (16.80)	–
Cu-guanine	Green	31.40 (31.41)	3.09 (3.09)	33.31 (33.31)	15.10 (15.09)	–

All of the complexes have melting points over 300 °C.

Table 2
Fundamental infrared bands (cm^{-1}) of adenine and its complexes

Adenine	Co^{II} complex	Ni^{II} complex	Cu^{II} complex	Assignment
3286, 3114	3340	3362	3327, 3180	ν_{NH_2}
2976	2970	2971	–	ν_{C-H}
2790, 2688, 2596	2629	2921, 2627	3630	ν_{N-H}
1668	1638	1638	1637	δ_{NH_2}
1601, 1502, 1446	1603, 1544, 1460	1545, 1462	1603, 1544	$\nu_{C=N}$, $\nu_{C=C}$ + ring
1451, 1365, 1331, 1307	1392, 1339, 1308	1391	1460, 1392, 1339, 1308	Vibrations
1250	1200	1212	1199	ν_{C-NH_2}, or δ_{N-H}
1025	1045	1048	1043	ρ_{NH_2}
	341.3	341	341	ν_{M-O}
	231	231	231	ν_{M-N}

as large as those corresponding to N-bonded complexes of this ligand. So, the NH_2 group (exocylic NH_2 nitrogen), is coordinated to the metal ion in the complexes. Adenine presumably coordinates through ring nitrogen with appreciable shifts and occasional splitting of $\nu_{C=C}$, $\nu_{C=N}$ and ring vibrations of the ligand (1605–1300 cm^{-1}) [19–25]. The ν_{NH} region, 2900–2500 cm^{-1}, suffered considerable changes in the Co^{II}, Ni^{II} and Cu^{II} complexes resulting of two weak maxima in this region. The 1250 cm^{-1} of adenine due to ν_{C-NH_2} or δ_{N-H} ring mode shifts to lower wavelength upon complexation. The bands at 1045, 1048 and 1043 cm^{-1} in Co^{II}, Ni^{II} and Cu^{II} complexes (Table 2), respectively, are due to ν_{NH_2}. This facilitates that adenine is binding exclusively through ring nitrogen [19]. The copper atom in the Cu-adenine complex lies on a crystallographic two fold axis, the four coordination sites being accepted by two chlorides and the N(9) atoms of two adenine cations [26]. The reported Cu–Cl and Cu–N distances of 2.228 and 2.012 Å, respectively are normal. The Cl–Cu–Cl, Cl–Cu–N, N–Cu–N and two independent bond angles subtended at copper by coordinated ligands are 97.78, 93.80, 94.74 and 144.66°, respectively [26]. There is no close approach of any atom to the copper centre. There are weak Cl···Cl interactions of length 3.755 Å which link one copper centre to those above and below it from infinite zigzag polymeric chains with Cu–Cl···Cl bond angle of 169.33°, while these Cl···Cl separations might normally be considered large. The $[Cu(H_2L)Cl_2]^{2+}$ monomers would also be expected to provide pathway for magnetic exchange. The $Cu(L)_2{\cdot}4H_2O$ complex contains the diameric unit $Cu_2(L)_4(H_2O)_2$ [27], with a structure similar to that of copper acetate with four binding adenine anions coordinated through N and water occupying axial sites.

The complex $Cu(HL)Cl_2$ prepared in solutions which are only slightly acidic contains neutral adenine as a ligand [28]. The magnetic susceptibility of this complex exhibits a maximum at 55 K and the complex is diamagnetic below 10 K [38]. The magnetic results clearly demonstrate the presence of exchange coupled copper dimers and thus a ligand-bridged structure is required. However, the studied complexes gave new IR bands at 341 and 231 cm^{-1} corresponding to ν_{M-O} and ν_{M-N}, respectively. The electronic absorption spectra of the separated solid complexes showed characteristic bands at (500, 665), (655, 850) and 560 nm with magnetic moments of 4.49, 3.67 and 1.19 BM for Co^{II}, Ni^{II} and Cu^{II} complexes, respectively (Table 3), depicting their existence in tetrahedral geometries [28].

Table 3
Nujol mull electronic absorption spectra δ_{max} (nm) and effective magnetic moment values (ν_{eff}, BM at 298 K) for the adenine complexes

	Co^{II} complex	Ni^{II} complex	Cu^{II} complex
δ_{max}	500, 655	655, 850	560
ν_{eff}	4.49	3.67	1.19

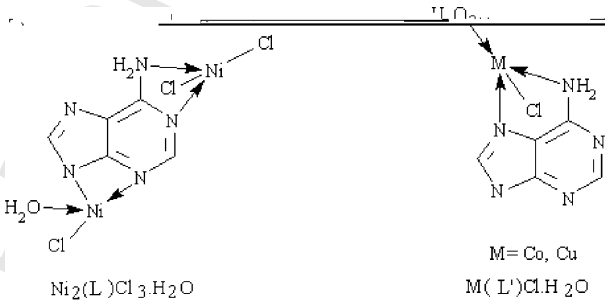

3.2. Spectral and magnetic identification of guanine complexes

The IR spectra of the free guanine and its complexes are collected in Table 4. Guanine exhibits bands at 3320, 1630, 780, 735 and 500 cm^{-1} which are due to the different modes of vibrations of the NH, ν, δ and ρ. On complexation, these bands are not affected indicating that the amino group is not involved on complexation. The ligand gave strong splitted carbonyl bands at 1695, 1670 cm^{-1} corresponding to the $\nu_{C=O}$ of the amide. However, these two bands and the $\gamma_{C=O}$ band of the ligand at 580 cm^{-1} are shifted towards lower wave number by about 10 and 30 cm^{-1}, respectively, on complexation indicating that the C=O group is either involved on the structural configuration

Table 4
Fundamental infrared bands (cm^{-1}) of guanine and its complexes

Ligand	Cobalt(II) complex	Nickel(II) complex	Copper(II) complex	Assignment
3440(b)	3440(w.sh)	3440(w.sh)	3440(w)	ν_{OH}
3320(s)	3320(s)	3320(s)	3320(s)	ν_{NH} of amino
3120(s)	3120(s)	3120(s)	3120(s)	ν_{NH} of amide
2980(sh)	2990(sh)	2980(sh)	2980(sh)	
2910(m)	2910(m.b)	2910(m.sp)	2910(m.sp)	ν_{C-H}
2840(sh)	2840(w)	2840(sh)	2840(sh)	
2690(m.b)	2690(m)	2690(m)	2690(m)	N(9)–H stretching vibration
2450(sh.w)	2450(sh.w)	2450(sh)	2450(sh)	
1695(sp.s)	1680(sp.s)	1685(sp.s)	1685(sp.s)	$\nu_{C=O}$
1670	1655	1655	1655	
1630(sh.w)	1630(v.sh)	1630(w.sh)	1630(w.sh)	δ_{N-H} of amide
1565(s)	1560(s.b)	1560(b.s)	1560(b.s)	
1505(v.w)	–	1505(v.w)	1505(v.w)	ν_{N-H} of amide
1475	1470(sp.m)	1470(sp.m)	1470(sp.m)	
1460(sp.m)	1455	1460	1460	
1415(m)	1400(m)	1400(m)	1400(m)	ν_{C-N} of amide
1375(v.s)	1370(v.s)	1370(v.s)	1370(v.s)	
1260(v.s)	1260(s)	1260(v.s)	1260(v.s)	
1215(s)	1215(s)	1215(s)	1215(s)	
1175(s)	1170(s)	1170(s)	1170(s)	ν_{C-NH} of amino
1150(w)	1145(w)	1145(w)	1145(w)	
1120(s)	1110(s)	1110(s)	1110(s)	ν_{C-OH}
1050(w)	1040(w)	1040(w)	1040(w)	
955(v.s)	955(v.s)	955(v.s)	955(v.s)	Ring vibration
885(s)	880(s)	880(s)	880(s)	
855(s)	850(b.s)	850(s)	850(s)	γ_{OH}
845(sh)	840(b.s)	840(w.sh)	840(w.sh)	
780(s)	780(s)	780(s)	780(s)	γ_{NH} of amino
735(v.w.sh)	735(sh.w)	735(w.b)	735(w.b)	
705(m.sp)	705(m.sp)	700(m.sp)	700(m.sp)	γ_{C-OH}
690(m)	670(m)	670(m)	670(m)	γ_{C-OH}
650(m)	645(m)	645(m)	645(m)	
605(m)	605(w)	605(m)	605(m)	$\gamma_{C=O}$
580(sh.b)	550(sh.b)	550(b.m)	550(b.m)	
500(w)	505(b.w)	500(m)	500(m)	ρ_{NH} of amide
400(s)	400(s)	400(m)	400(s)	ρ_{NH} of amino
–	–	–	345(s)	M–Cl

of the complex or the phenomenon of tautomerism is assigned. The ligand and the complexes showed ν_{OH} bands at 3440 cm^{-1}, indicating that the ligand existed in a keto-enol form. The band corresponding to ν_{C-N} (amide) in the free ligand, at 1415 cm^{-1} is shifted on complexation, i.e. the C–N^7 of the five membered ring in guanine is involved on the complexation. This indicates that N(7) is more donating than N(3), because of the resonance stabilization of N(7).

The Nujol mull electronic absorption spectra of the guanine complexes for Co^{II}, Ni^{II} and Cu^{II} complexes (Table 5) gathered with that of effective magnetic moment values (Table 5) indicated the high-spin octahedral geometry of all complexes [39]. So the following structures are postulated

Table 5
Nujol mull electronic absorption spectra δ_{max} (nm) and effective magnetic moment values (ν_{eff}, BM at 298 K) of the guanine complexes

Complex	δ_{max} (nm)	ν_{eff}
Co-guanine	696(sh), 587(sh), 413(s), 312(s)	5.2
Ni-guanine	853(sh), 743(w.b), 416(s), 286(s), 262(sh)	2.1
Cu-guanine	683(v.b), 423(sh), 409(s), 355(w), 313(s)	2.52

for the prepared complexes:

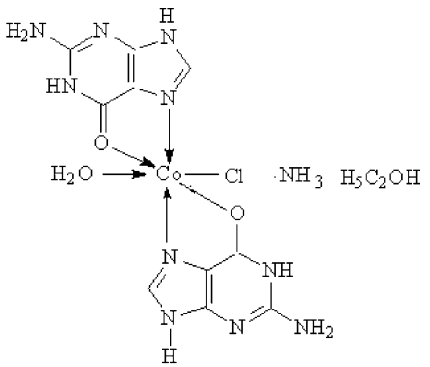

$[Co(H_2L')Hl\ Cl\ H_2O].NH_3.C_2H_5OH$

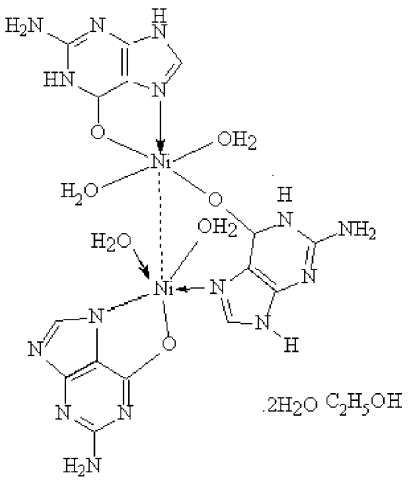

$[Ni(HL')_2L'(H_2O)_4].H_2O.C_2H_5OH$

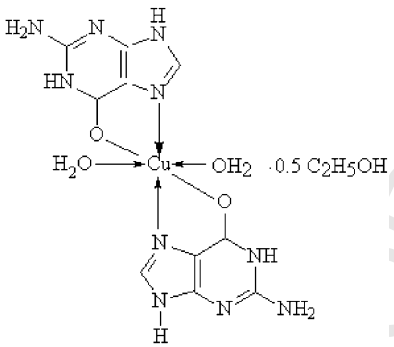

$[Cu(HL')_2(H_2O)_2]\ 0.5C_2H_5OH$

Table 6
Coordination bond lengths of pyrimidine–metal complexes

Compound	r (A)
Co[adenine] $Cl{\cdot}H_2O$	2.25
Ni_2[adenine] $Cl_3{\cdot}H_2O$	2.23
Cu[adenine] $Cl{\cdot}H_2O$	2.18

3.3. Bonding in adenine complexes

The coordination bond length r can be determined from the relation [30,31]:

$$\Delta\nu = \frac{32\pi\alpha}{a^2}\frac{\nu_{x=y} - \nu_{x-y}}{I}\exp(-2\pi\sqrt{(2r/a)}$$

where α is the bond polarisability, $\Delta\nu$ the shift in the oscillator frequency, a the lattice constant of the metal salt (a = 3.5, 3.524 and 3.614) for cobalt, nickel and copper, respectively [32], ν_{x-y} the frequency of the oscillator with single bond, $\nu_{x=y}$ the frequency of the oscillator with double bond and I is the length of the oscillator coordinated to the metal ion (I = 1.905 and 1.993 for cobalt [33], nickel [30] and copper [30], respectively. The values were computed based on a published data [34]. These are 48.61, 46.59 and 42.50 for cobalt, nickel and copper, receptively. From such data, the r values between the metal and the nitrogen atom of the C=N group are computed (Table 6). It seems that the copper complexes are with shorter coordination bond length than those of cobalt and nickel complexes. This could be attributed to the increase in the strength of the electrostatic field of the copper ion as a result of the smaller ionic radius of the Cu^{II} ion compared to that of Ni^{II} or Co^{II} ions, i.e. the electronic configuration of the element affects such trend.

3.4. ESR of copper complexes

It is possible to measure the covalent band character α^2, where α is the coefficient of the ground state of $d_{x^2-y^2}$ orbital, from the expression [26–37]:

$$\alpha^2 = \frac{A_{11}}{0.036} + (g_{11} - 2.0023) + \frac{3}{7}(g_{\perp} - 2.0023) + 0.04$$

A_{11} is the parallel coupling constant (cm^{-1}). The α^2 value for Cu^{II} complexes with tetragonal distortion lies in the range of 0.63–0.84 for nitrogen donor ligands [38] and 0.84–0.94 for oxygen donor ligands [39]. Axial ligands cause changes in equatorial bond length and hence g and A values [40]. Bonding between ligands and Cu^{II} ion occurs through the 4s and 4p orbitals of the Cu^{II} ion with the ligand orbitals. The presence of apical ligands introduces 4s character in the ground state which decreases the contact hyperfine interaction. Therefore, if the 4s character in the ground state is known, it is possible to know the axial field strength in the presence of small percentage of 4s character in the ground state, the fraction of the 3d character in the CuII 3d–4s

Table 7
ESR parameters for copper-adenine and guanine complexes

Complex	g_{11}	$g_{\perp}$	<g>	G	A_{11}	$A_{\perp}$	α^2	f^2
Cu-guanine	2.23	2.05	2.11	4.60	88	38	0.52	0.80
Cu-adenine	2.11	2.03	2.06	3.66	185	18.5	0.67	0.98

ground state, f^2, can be determined from the following equation [36]:

$$\alpha^2 f^2 = \frac{7}{4}\left[\frac{A_{11}}{0.036} - \frac{A}{0.036} + \frac{2}{3}g_{11} - \frac{5}{21}g_{\perp} - \frac{6}{7}\right]$$

The room temperature poly crystalline X-band ESR spectral pattern of the Cu-adenine and Cu-guanine complexes (Table 7) gave similar pattern. Both are of anisotropic nature. The spectral analysis of these complexes gave two values g_{11} 2.11 and 2.23 and $g_{\perp}$ 2.03 and 2.05 for both adenine and guanine complexes, respectively. The calculated <g> values $= (g_{11} + 2g_{\perp})/3$ are 2.06 and 2.11, respectively. The lowest g value was more than 2.00 consequently, to assign the tetragonal distorted symmetry associated with $d_{x^2-y^2}$ ground state rather than d_{z^2} [41]. The G values were 3.66 and 4.60 for adenine and guanine complexes, indicating weak Cu–Cu interaction in the adenine complex and no Cu–Cu interaction in the guanine complex. The A_{11} values for the two complexes were 185 and 88, indicating the probability of the pseudo T_d structure around Cu ion in the guanine complex; where the value of $A_{11} < 100$ [35]. The calculated α^2 and f^2 values (Table 7) indicated the stronger axial field in the adenine complex. From the values of α^2 one can say that the metal–ligand bond in the guanine complex is less covalent than that of adenine. Generally, the difference in the ESR spectral data of the Cu-adenine and Cu-guanine complexes may attribute to the difference in the geometry of the two complexes, i.e. T_d and O_h, respectively.

3.5. Thermal analysis

3.5.1. Adenine complexes

Differential thermal analysis of these complexes (Table 8) gave the following features.

1. The DTA pattern of Co-, Ni- and Cu-adenine complexes indicated that there is a great similarity in their thermal behaviour. Each complex gave one exothermic broad band at a temperature higher than 250 °C indicating the higher stability of these complexes up to this temperature.
2. The activation energy changes of the decomposition step for the complexes were in the order Co-adenine < Cu-adenine < Ni-adenine complexes. Such order is reversed to the maximum temperature of the decomposition step, i.e. the decomposition steps of these complexes are thermodynamically controlled.
3. The fractions appeared in the calculated order of the thermal decomposition steps indicated that these thermal steps are not kinetically simple.
4. The narrow range of the entropy changes (−0.22 to −0.24) illustrated the similarity of the thermal behaviour. The negative sign indicated that the transition states of the thermal reaction are more ordered.
5. The values of the enthalpy changes have a similar trend as that of the entropy changes.
6. The thermal gravimetric analysis indicated that the products of the residual decomposition complexes are the metal oxides.

3.6. Guanine complexes

The DTA curve of octahedral cobalt guanine complex, $[Co(H_2L')HL'H_2O]\cdot NH_3\cdot C_2H_5OH$, exhibits six endothermic peaks in the temperature range 310.0–976.0 K (Table 9). The first and the second weak endothermic peaks in the temperature range (310.0–404.5 and 404.5–491.8 K) are assigned to the desolvation of $1C_2H_5OH$ and $1NH_3$ molecules, respectively. This is strongly supported by the TG measurements, which gave weight loss exactly equivalent to $1C_2H_5OH$ and $1NH_3$ molecule. The TGA curve displays the observed weight loss 7.5% in the temperature range (491.8–704.3 K), which is probably due to replacement of HCl molecule (calcd. 7.7%). The DTA and TGA curves depicted that as the HCl is removed, the complex is decomposed. The third strong endothermic peak in the temperature range (704.3–798.6 K) could be argued to the first step of the decomposition. This is confirmed by the observed TG weight loss 43.5% equivalent to $3N_2$, $2CH_2{=}C{=}CH_2$ and H_2O (calcd. 44.1%). The fourth endothermic peak in the temperature range (98.6–843.0 K) is due to the second decomposition step, as evident from the observed TG weight loss 10.9% equivalent to 2C=N (calcd. 10.9%). On the other hand, the fifth endothermic peak in the temperature range (843.0–925.0 K) and the TG measurements illustrated the following processes.

(i) The observed weight loss (14.6%) is equivalent to 2N, 2C and H_2O at 843.0–885.0 K (calcd. 14.7%).

Table 8
DTA parameters of the adenine complexes

Compound	Type	T_m (K)	ΔE_a (kJ mol^{-1})	n	α_m	$\Delta S^{\#}$ (kJ mol^{-1})	$\Delta H^{\#}$ (kJ mol^{-1})	Z	Assignment
$Co[adenine]Cl\cdot H_2O$	Endo	660	121.94	1.16	0.60	−0.24	−156.41	5.746	Formation of CoO
$Ni_2[adenine]Cl_3\cdot H_2O$	Endo	508	323.08	0.59	0.72	−0.22	−113.57	22.23	Formation of NiO
$Cu[adenine]Cl\cdot H_2O$	Endo	603	231.35	2.52	0.46	−0.23	−138.57	12.45	Formation of CuO

Table 9
DTA and TGA analysis of guanine complexes, guanine = HL

Complex	Type	T_m (K)	ΔE (kJ mol^{-1})	n	α_m	$\Delta S^{\#}$ (kJ mol^{-1})	$\Delta H^{\#}$ (kJ mol^{-1})	$10^3 Z$ (s^{-1})	Temperature range	Loss (wt.%)		Assignment
										Calculated	Found	
$Co(HL)_2 \cdot OC_2H_5Cl \cdot H_2O \cdot NH_3$	Endo	350.55	25.27	1.35	0.58	−0.320	−112.1	1.45	310.0–404.5	3.9	4.0	Dehydration of C_2H_5OH
									404.5–491.8	3.6	3.6	Dehydration of NH_3
										7.7	7.5	Replacement of HCl
	Endo	781.99	119.72	0.69	0.7	−0.320	−250.38	3.07	491.8–704.3	44.1	43.5	Decomposition of $3N_2$, H_2O, $2CH_2{=}C{=}CH_2$
	Endo	817.46	34.67						704.3–798.6			
				1.63	0.54	−0.331	−276.76	0.85	798.6–843.0	10.9	10.9	Decomposition of 2C=N
	Endo	868.51	428.17	2.08	0.49	−0.311	−270.4	9.88	843.0–925.0	14.7	14.6	Decomposition of 2N, 2C, H_2O
										15.7	15.8	Formation of CoO
	Endo	945.1	599.77	2.34	0.47	−0.310	−292.91	0.013	935.0–976.0	13.7	13.8	Formation of Co + 0.4(O)
$Ni_2L_3 \cdot OC_2H_5 \cdot 5H_2O$	Endo	354.63	25.86	1.59	0.54	−0.320	−113.4	1.46	323.0–398.0	1.25	1.38	Dehydration of $H_2O + C_2H_5OH$
	Endo	619.05	133.02	0.99	0.63	−0.315	−195.26	4.31	398.0–635.5	3.75	3.75	Dehydration of H_2O
	Endo	777.88	144.66	0.73	0.69	−0.319	−274.78	3.73	704.3–791.0			
	Endo	814.66	162.12	1.21	0.6	−0.318	−259.34	3.99	791.0–841.0	22.5	22.4	Formation of 2NiO + 0.5(O) as a final product
	Endo	895.35	199.54	1.17	0.60	−0.318	−284.89	4.47	841.0–938.0			
$CuL_2 \cdot 2H_2O \cdot 0.25C_2H_5OH$	Endo	307.33	70.67	2.78	0.44	0.309	−94.98	4.61	303.0–438.0	2.72	2.75	Loss of $0.25C_2H_5OH$
	Endo	367.33	138.59	1.26	0.59	−0.306	−112.55	7.56				
	Exo	531.1	236.95	1.52	0.55	−0.308	−163.62	8.94	438.0–663.0	11.10	11.24	Loss of $2H_2O$ and $0.25C_2H_5OH$

(ii) The decomposition process with 15.8% is equivalent to CoO at 885.0 K (calcd. 15.7%).

(iii) The formed metal oxide started to lose oxygen temperature ranges (885.0–935.0 K). The DTA endothermic peak in the temperature range (935.0–976.0 K) is due to the formation of Co + 0.4 (○) as evident from TGA curve, where the observed value becomes 13.8 % compared to the calculated value 13.7%.

In summary, the mechanism of the cobalt guanine complex could be given in the following steps:

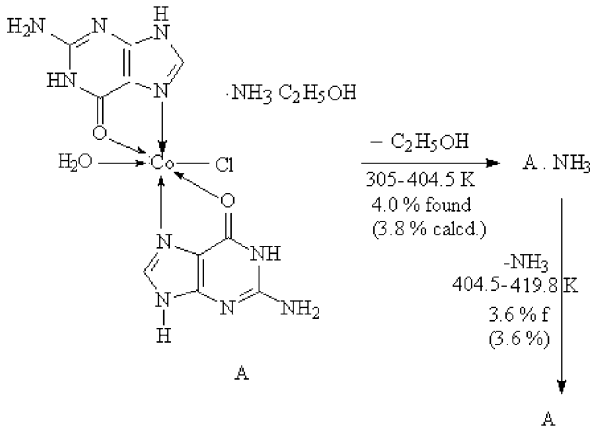

Then the dissociation of A:

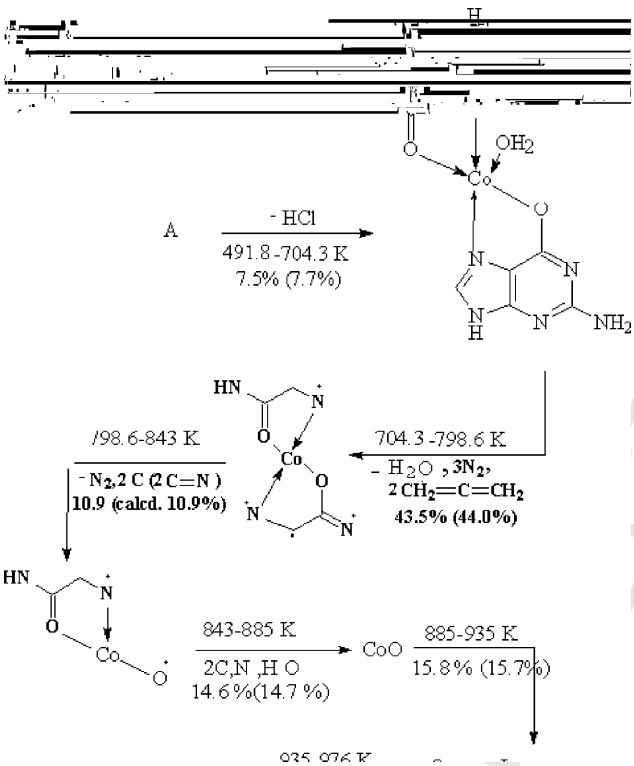

The order of reaction and the activation energy of different kinetic steps were calculated and the data are collected in Table 9. The first step of the decomposition reaction is of a pseudo first order kinetics while the second step proceeds in second order conditions.

The DTA curve of the octahedral nickel guanine complex, $[Ni(HL')_2L'(H_2O)_4]\cdot H_2O\cdot C_2H_5OH$ exhibits five endothermic peaks in the temperature range (323–929 K). The first two weak endothermic peaks in the temperature ranges (323.0–398.0 and 398.0–635.5 K) are assigned to be the loss of crystallization molecules as evident from the TG observed weight loss (5.13%) equivalent to one water and one alcohol molecules (calcd. 5.01%) where the solvents are trapped in the crystal voids. The activation energies and the order of the desolvation reaction are 25.86 kJ mol^{-1}, $n = 1.59$ and 133.02 kJ mol^{-1}, $n = 0.996$ for the first and second peaks, respectively (Table 9). The DTA curve shows loss in energy in the temperature range (636.5–704.3 K), corresponding to the observed TG weight loss 4.9% equivalent to the loss of the coordinated water molecules (calcd. 5.1%). This is confirmed from the TGA curve. The third, fourth and fifth endothermic DTA peaks in the temperature ranges 704.3–791, 791–841 and 841–938 K, respectively, are due to vigorous decomposition process. The TGA curves proved such view: 2NiO + 0.5O as final products. The orders of the reactions for these peaks are 0.73, 1.21, 1.17, respectively, i.e. the decomposition of the complex follows the first order reaction mechanism. The DTA and TGA curves of the octahedral copper guanine complex, $[Cu(HL')_2(H_2O)_2]\ 0.5C_2H_5OH$, gave two weak endothermic peaks in the temperature ranges (303.0–438.0 K), corresponding to the observed TG weight loss (2.75%), equivalent to 0.25 ethanol molecule (calcd. 2.72%) exists as crystal voids. Following the process of the decomposition in the temperature ranges (438.0–703.0 K). The DTA curve exhibits an exothermic peak. The TGA data pointed to that the observed TG weight loss (11.24%) is equivalent to the weight loss of $2H_2O$ and $0.25C_2H_5OH$ molecules (calcd. 11.1%) in the temperature range (438.0–663.0 K). The solvent molecules ($0.25C_2H_5OH$ and $2H_2O$) are in the lattice structure and in the coordinated sphere of the complex, respectively. The final product of the thermal decomposition of the complex is copper metal. The change of entropy, $\Delta S^{\#}$, values for all complexes (Table 9) are nearly of the same magnitude and lie within the range −0.305 to −0.331 kJ K^{-1} mol^{-1}. So, the transition states are more ordered, i.e. in a less random molecular configuration, than the reacting complex[185]. The fraction appeared in the calculated order of the thermal reaction, n (Table 9) confirmed that the reactions proceeded in complicated mechanisms. The calculated values of the collision number, Z, showed a direct relation to the activation energy ΔE. The peak temperature, T_m, at which the peak is maximum or minimum, defines the position of the peak. The values of the decomposed substance fraction, α_m, at maximum development of the reaction were calculated (Table 9). It is nearly of the same magnitude and lies within the range (0.44–0.71). The change of the heat of transformation, $\Delta H^{\#}$, can be calculated from the DTA curves. In general, the $\Delta H^{\#}$ for any phase transformation taking place at any peak temperature, T_m, can be given by the following

Table 10
Electrical conductivity parameters of adenine and guanine complexes

Complex	Region	ΔE (eV)	$\log \sigma^{\circ}$ (Ω^{-1} cm^{-1})	Transition temperatures
Co-adenine	A	1.464	7.8	571.43
	B	0.475	8.7	526.32
	C	0.043	9.6	473.93
	D	−0.119	10.1	425.35
	E	−0.277	9.35	
Ni-adenine	A	1.765	7.6	571.43
	B	0.232	9.6	476.19
	C	−0.269	11.0	369.00
	D	0.102	8.7	
Cu-adenine	A	1.492	6.8	529.10
	B	0.250	9.4	438.09
	C	0.011	10.2	370.37
	D	−0.179	11.5	331.13
	E	0.073	9.4	
Co-guanine	A	0.604	8.75	480.77
	B	−0.198	10.3	711.52
	C	−0.784	12.6	334.45
	D	−1.112	8.1	
Ni-guanine	A	1.279	8.4	578.03
	B	0.083	9.9	483.09
	C	−0.851	12.6	392.16
	D	−0.239	9.24	322.58
	E	0.031	7.4	
Cu-guanine	A	2.104	5	496.89
	B	0.462	7.3	371.75
	C	−0.159	10.3	

equation:

$$\Delta S^{\#} = \frac{\Delta H^{\#}}{T_{\mathrm{m}}}$$

where $\Delta S^{\#}$ is the entropy of activation.

3.7. Electrical conductivity measurements

The dependence of the electrical conductivity on temperature is expressed by the following equation $\sigma = \sigma^{\circ} \mathrm{e}^{\Delta E/KT}$, where ΔE is the activation energy for the conduction, σ° is a constant for the conductivity independent of the temperature and K is the Boltzmann constant. The electrical conductivity data are collected in Table 10. The data depict that all complexes are of semi-conductor behaviour. The magnitude of ΔE can be affected by the ambient atmosphere, the presence of impurities and pressure. The discontinuation in the complexes in the conducting curves can be argued to be a molecular rearrangement or crystallographic transition due to traps formation or delocalization. Such case is familiar for complexes with semi-conductor behaviour.

The electrical conductivity pattern of the Co-, Ni- and Cu-adenine complexes showed five, four and five regions, respectively, with transition temperatures 571.43, 526.32, 473.93, 425.35, 571.43, 476.19, 369.00 and 529.1, 483.09, 37.37, 331.13 K, respectively. The activation energies are within the range of −0.269 to 1.464 eV. The data revealed the semi-conducting behaviour of these complexes. The $\Delta E - \log \sigma^{\circ}$ relation for the adenine complexes gave the following empirical equation: $\Delta E = -1.579 \log \sigma^{\circ} + 0.984$.

The electrical conductivity patterns of (1:2) cobalt, (2:3) nickel and (1:1) copper complexes of guanine showed four, five and three regions, respectively, with transition temperatures of 480.77, 411.52 and 334.45, 578.03, 483.09, 392.16 and 322.58, and 496.89 and 371.75 K, respectively, and activation energies ranged from −0.112 to 2.164 eV. Regions B–D, and B and C of Co and Cu complexes, respectively, are due to the desolvation process of the complexes and region A is due to the partial decomposition of the complexes. Whereas, in case of nickel complex, all the five regions are due to the desolvation process of the complex (Table 10). The $\Delta E - \log \sigma^{\circ}$ curve gave the following empirical equation for the conduction of the studied guanidine complexes: $\Delta E = -2.172 \log \sigma^{\circ} + 9.559$.

References

[1] L.J. Berliner, S.S. Wong, Biochemistry 14 (1975) 4977.
[2] L. Grossman, A. Braun, R. Feldberg, I. Mahler, Ann. Rev. Biochem. 44 (1975) 19.
[3] S. Ljungquist, T. Lindahl, J. Biol. Chem. 249 (1974) 1530.
[4] G.L. Eichhorn, in: G. L. Eichhorn (Ed.), Inorganic Biochemistry, vol. 2, Elsevier, New York, 1973, p. 1191, 1210.
[5] M.S. Masoud, S.S. Haggag, Thermochim. Acta 196 (1922) 221.
[6] M.S. Masoud, S.A. Abou El-Enein, O.F. Hafez, J. Thermal Anal. 38 (1992) 1365.
[7] M.S. Masoud, Z.M. Zaki, F.M. Ismail, A.K. Mohamed, Z. Fur Phys. Chem. 185 (1994) 223.
[8] M.S. Masoud, O.H.A. El-Hamid, Z.M. Zaki, Trans. Met. Chem. 19 (1994) 21.
[9] M.S. Masoud, S.S. Haggag, Z.M. Zaki, M. El-Shabasy, Spectrosc. Lett. 27 (1994) 775.
[10] M.S. Masoud, A.A. Hasanein, A.K. Ghonaim, E.A. Khalil, A.A. Mahmoud, Z. Fur Phys. Chem. 209 (1999) 223.
[11] M.S. Masoud, E.A. Khalil, A.A. Ibrahim, A.A. Marghany, Z. Fur Phys. Chem. 211 (1999) 13.
[12] M.S. Masoud, H.H. Hamoud, Ultra Sci. Phys. Sci. 12 (2000) 12.
[13] M.S. Masoud, A.K. Ghonaium, R.H. Ahmed, A.A. Mahmoud, A.E. Ali, Z. Fur Phys. Chem. 513 (2000) 215.
[14] M.S. Masoud, A.K. Ghonaim, R.H. Ahmed, S.A. Abou El-Enein, A.A. Mohamed, J. Coord. Chem. 55 (2002) 79.
[15] A.I. Vogel, A Text Book of Quantitative Inorganic Analysis, fourth ed., Longmann, London, 1978, p. 116, 452.
[16] P.H. Lee, E. Griswold, J. Kleinberg, Inorg. Chem. 3 (1964) 1278.
[17] D. Reinen, G. Friebel, Inorg. Chem. 23 (1984) 791.
[18] N.B. Figgs, J. Lewis, Modern Coordination Chemistry, Interscience, New York, 1967, p. 403.
[19] S. Shirotake, Chem. Pharm. Bull. 28 (1980) 1673.
[20] R. Savoic, J.J. Jutier, L. Prizant, A.L. Beauchamp, Spectrosc. Chim. Acta 38 (1982) 561.
[21] J. Brigando, D. Colitis, M. Morel, Bull. Soc. Chem. Fr. 3445 (1969) 3449.
[22] T. Fujita, T. Sakaguchi, Chem. Pharm. Bull. 25 (1977) 1055.
[23] A.N. Speca, C.M. Mikulski, F.J. Iaconianni, L.L. Pytlewski, N.M. Karayannies, J. Inorg. Nucl. Chem. 43 (1981) 2771.

[24] A.N. Speca, L.L. Pytlewski, C.M. Mikulski, N.M. Karayanni, Inorg. Chim. Acta 66 (1982) 153.
[25] A. Lautie, A. Novak, J. Chem. Biol. 65 (1968) 1359.
[26] D.B. Brawn, J.W. Hall, H.M. Helis, E.G. Walton, D.J. Hodgson, W.E. Halfield, Inorg. Chem. 16 (1977) 2675.
[27] E. Sletten, Acta Crystallogr. B 25 (1969) 1480.
[28] R. Weiss, H. Venner, H. Seyler, Z. Physiol. Chem. 33 (1963) 169.
[29] W. Levason, C.M. MacAulife, Inorg. Chim. Acta 14 (1975) 127.
[30] S.C. Bhtia, J.M. Bindlish, A.R. Saini, P.C. Jain, J. Chem. Soc., Dalton Trams. (1981) 1773.
[31] G. Karagonins, O. Peter, Z. ElectroChem. Ber. Eunsenges Phys. Chem. 63 (1959) 1170.
[32] C.H. Macgillavery, G.D. Rieckin, in: K. Lonsdale (Ed.), International Tables for X-ray Crystallography: Physical and Chemical Tables, vol. 3, 1962.
[33] I. Saski, D. Pujol, A. Gauderner, A. Chiaroni, C. Riche, Polyhedron 6 (1987) 2103.
[34] R.K. Parasher, R.C. Sharma, A. kumar, G. Hohan, Iinorg. Chim. Acta 72 (1988) 201.
[35] D. Kirelson, R. Neiman, J. Chem. Phys. 35 (1961) 149.
[36] H.A. Kuska, M.T. Rogers, R.E. Drullinger, J. Phys. Chem. 71 (1967) 109.
[37] J.I. Zink, R.S. Drago, J. Am. Chem. Soc. 94 (1972) 44550.
[38] D.R. Lorenz, J.R. Wasson, D.K. Johonson, D.A. Thorpe, J. Inorg. Nucl. Chem. 37 (1975) 2297.
[39] D.K. Johonson, H.J. Stklosa, J.R. Wasson, W.L. Seebach, J. Inorg. Nucl. Chem. 37 (1975) 1397.
[40] B.A. Stastry, S.M. Asdullah, G. Ponticelli, M. Massacesi, J. Chem. Phys. 70 (1979) 2834.
[41] M.H. Sonar, A.S.R. Murty, J. Inorg. Nucl. Chem. 42 (1980) 815.